Journal of Materials Chemistry B

ROYAL SOCIETY OF CHEMISTRY

PAPER

View Article Online
View Journal | View Issue

Check for updates

Cite this: J. Mater. Chem. B, 2025, 13, 11032

Multifunctional bio-inspired biomedical adhesive featuring fast-acting adhesion for topical drug delivery†

Jacob Boykin, [a] Nina Zamani, [b] Akash Gunjan *[b] and Hoyong Chung *[a]

Received 24th January 2025,
Accepted 14th July 2025

DOI: 10.1039/d5tb00175g

rsc.li/materials-b

This report presents the synthesis and characterization of a new biomedical adhesive featuring fast-acting adhesion properties for potential application in topical drug delivery to localized areas. This new biomedical adhesive is synthesized through thermally initiated radical polymerization and consists of: (1) a mussel-inspired repeating unit (catechol), which provides strong biomedical adhesion, biocompatibility, and robust skin interactions, and (2) 2-acrylamido-2-methyl-1-propanesulfonic acid (AMPS), an anionic repeat unit known for its biocompatibility, drug delivery capabilities, and electrostatic interactions. This combination leads to a multifunctional biomedical adhesive that offers fast-acting adhesion to the skin without the need for additional crosslinkers. The resulting copolymer, poly(2-acrylamido-2-methyl-1-propanesulfonic acid-*co*-*N*-methacryloyl 3,4-dihydroxyl-L-phenylalanine), further known as poly(AMPS-*co*-MDOPA), was tested both on PET films and porcine skin to quantify the adhesion properties and compare the setting times of the adhesive. A small amount (30 mg on dry PET surface, 100 mg on wet porcine skin) of adhesive was able to achieve a maximum strength of 105 kPa on a dry PET substrate in a lap shear strength test, and 3.1 kPa on wet porcine skin following only 5 minutes of application time. ^{1}H NMR was performed to confirm the chemical structure of the polymer, demonstrating successful synthesis with a repeating unit ratio of 88 : 12 for AMPS : MDOPA. The polymer showed no significant cytotoxicity when exposed to primary human dermal fibroblasts at modest concentrations, proving the polymers' excellent biocompatibility. In separate tests, the new polymer demonstrated significantly lower cytotoxicity compared to a commercial sunscreen approved for use on human skin. In tests using proliferating human dermal fibroblast cells, the combination of the new poly(AMPS-*co*-MDOPA) (7.5 mg mL^{-1}) with sodium valproate (2 mM) effectively triggered cell death, demonstrating successful drug delivery. Due to high/fast-acting skin adhesion, soft nature, biocompatibility, and drug efficiency, this new copolymer shows great promise as a biomedical adhesive for skin tissue, offering a comfortable and efficient alternative to drug-containing topical ointments by extending the residence time of the drug at a localized skin site.

1. Introduction

Polymer-based biomedical adhesives, capable of bonding two distinct tissue surfaces together, have recently been extensively studied as an alternative treatment to traditional wound closure methods such as sutures and staples.[1–3] Simultaneously, they have also been implemented as hemostatic agents, wound healing promoters, drug delivery agents, sealants, and for electrical device applications.[4–7] There are multiple commercially available biomedical adhesives, including: (a) synthetically developed adhesives, such as cyanoacrylate, Dermabond, Surgiseal, and Pattex; and (b) protein-derived adhesives, such as fibrin, gelatin, and albumin-based glues. However, both commercial and non-commercial but published biomedical adhesives still possess multiple downsides.[3,8,9] For example, while cyanoacrylate glues have substantial adhesion strength, they are known to generate heat due to rapid polymerization *in situ*, and can become very stiff, leading to poor compatibility with soft tissues.[10] In addition, the degradation product, formaldehyde, of cyanoacrylates has proven to be toxic.[3,8] The main alternative to these cyanoacrylate glues is fibrin glues, a biomedical adhesive that utilizes factors XIIIa and fibrinogen to

[a] Department of Chemical and Biomedical Engineering, Florida State University, 2525 Pottsdamer Street, Building A, Suite A131, Tallahassee, Florida 32310, USA. E-mail: hchung@eng.famu.fsu.edu
[b] Department of Biomedical Sciences, Florida State University College of Medicine, 1115 West Call Street, Tallahassee, FL 32306-4300, USA. E-mail: akash.gunjan@med.fsu.edu

† Electronic supplementary information (ESI) available. See DOI: https://doi.org/10.1039/d5tb00175g

create adhesion on biological surfaces.[1] Notably, the fibrin glues have weaker adhesion strength than cyanoacrylate glues and are susceptible to virus transmission attributed to its formulation method. Moreover, the introduction of additional functionalities is challenging due to its complex chemical structure.[2,3,8,11] Considering the aforementioned bottlenecks, the present study intended to develop a non-toxic water-based adhesive featuring comparative properties to commercially available biomedical adhesives, while serving as a drug delivery carrier.

Along these lines, exploitation of wet adhesion properties of mussels has emerged as one of the promising solutions to the shortcomings of the commercial biomedical adhesives.[12–17] Mussels possess many mussel foot proteins (Mfps) that allow for strong wet adhesion to rocks while underwater. The main component of Mfps that provides strong wet adhesion is the catechol group present in Mfp-5.[12] This particular functional entity consists of a benzene ring bearing two hydroxyl groups, and can be extracted from mussels in the form of levodopa (L-DOPA).[12,18,19] The strong adhesion of the catechol groups on surfaces, regardless of the material they are made from, mainly stems from a diverse range of forces including (a) hydrogen bonding *via* hydroxyl (–OH) groups; (b) covalent bonding with $-NH_2$ or –SH through oxidation of alcohol towards the formation of quinone followed by Michael addition and Schiff base adducts; (c) π–π interaction between the benzene rings at the interface; (d) π–cation interactions between benzene and surface amines; and (e) metal coordination to the benzene ring (Fig. 1a).[3,20–26] These interactions made catechol groups an essential component for synthesizing biomedical adhesives with improved adhesion in wet environments, without increasing the overall toxicity of the polymer.[12,27,28] This is primarily due to the diverse array of functionalities available on the skin surface. For example, keratin on the skin is rich in amines, glutathione on the epidermis has cysteine-rich backbones with ample thiols, hydroxyl groups are extremely abundant such as in serine, threonine and tyrosine, as well as some amino acids containing benzene rings, such as tyrosine.[29–31]

The catechol moiety enhances interfacial adhesion properties significantly; however, it may also increase the overall adhesive polymer's stiffness, which can lead to a decrease in biocompatibility[32–34] due to mechanical strength mismatch. Ideally, a biomedical adhesive should be both strong and ductile, meaning that the adhesive may undergo large deformation by dispersing the mechanical stress throughout the polymer matrix. To then achieve both the strength and the ductility of an ideal biomedical adhesive, the use of a catechol moiety with an anionic vinyl monomer, 2-acrylamido-2-methyl-1-propanesulfonic acid (AMPS), can be a solution through exploitation of electrostatic interactions.[35] Herein, the electrostatic interactions are a form of interaction that occurs nearly instantaneously between opposing electric charges with a relative bond energy strength of approximately 25 kJ mol^{-1}.[36] For example, the sulfonate anion in AMPS can form an electrostatic interaction with the ammonium cation on the skin, as shown in Fig. 1a. The electrostatic interaction between AMPS and *N*-methacryloyl 3,4-dihydroxyl-L-phenylalanine (MDOPA) within the polymer matrix also enhances the overall cohesive strength of the polymer.

AMPS is an anionic biocompatible monomer that has been utilized for a variety of biomedical applications ranging from wound dressings, tissue engineering, and drug delivery. In addition, AMPS contains a sulfonate group capable of participating in electrostatic interactions within the polymer matrix with the amide moieties on both other AMPS and MDOPA repeat units.[37–41] Because electrostatic interactions form instantly upon contact between charges, these fast interactions can serve as an effective initial adhesion mechanism for adhesive-to-substrate contact. In contrast, covalent bond-mediated adhesion is slower, as it takes time for the actual chemical connection to form between the adhesive and the substrate.

As the largest human organ that is also in constant contact with the external environment, our skin has evolved several inbuilt protective features.[42] These include the epidermis, which is the protective outer layer of the skin which includes keratinocyte cells that secrete lipids and proteins such as keratin that aids in forming a water-proof layer to protect the underlying layers of tissue. Terminally differentiated keratinocytes eventually give rise to the layer of dead cells on the external surface of the epidermis to provide additional protection. Underneath the epidermis lies the dermis with its sebaceous glands that secrete a waxy material with waterproofing properties to further add to the protective features of the skin. Despite the presence of numerous features of the skin that would protect it and the underlying tissues from the toxic effects of substances applied on the skin, any polymeric adhesive designed for topical drug delivery needs to be first tested for potential toxicity toward skin cells. As a first step, this could be achieved simply by performing *in vitro* toxicity studies on skin fibroblasts cells in two dimensional (2-D) cultures.[43,44] More in-depth toxicity studies can be performed using *in vitro* three-dimensional (3-D) fibroblast cultures,[45] or testing by direct application *ex vivo* onto porcine[46] or human skin explants.[47] Finally, toxicity studies can also be performed *in vivo* on live hairless mice,[48] as on the skin of human volunteers,[49] but only if warranted following *in vitro* and/or animal studies.

In this study, we present a newly developed biomedical adhesive – a copolymer comprising AMPS and MDOPA. This biomedical adhesive exhibits high biocompatibility, drug loading properties, hydrophilicity, fast-acting adhesion formation, along with strong adhesion properties. The pendant catechol groups offer substantial wet adhesion, as the anionic sulfonate engages in additional ion–dipole interaction (*i.e.*, electrostatic interaction) with the tissue surface. Furthermore, the anionic sulfonate pendant on the polymer can be harnessed for valproate drug delivery to primary human dermal fibroblasts by forming an electrostatic complex. Overall, this study presents a novel biomaterial that offers multifunctionality, such as drug delivery, in addition to the traditional roles of a biomedical adhesive.

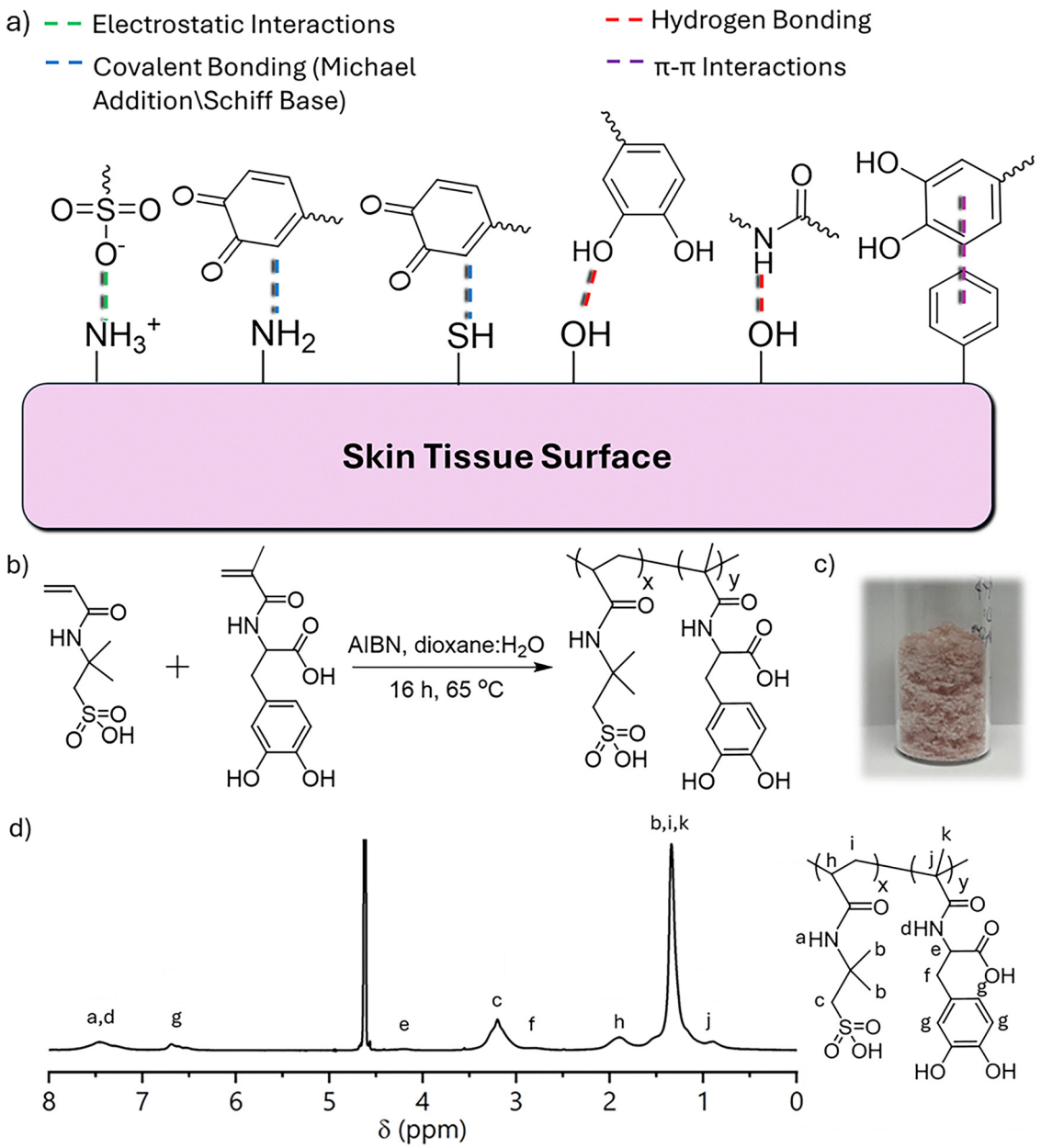

Fig. 1 (a) Available skin tissue functional group adhesion mechanisms of poly(AMPS-*co*-MDOPA) chemical moieties onto skin tissue (concentration of functional groups shown may vary on location). (b) Chemical scheme of poly(AMPS-*co*-MDOPA) synthesis. (c) A photo of dried poly(AMPS-*co*-MDOPA) following lyophilization to powder form. (d) ^{1}H NMR spectrum of poly(AMPS-*co*-MDOPA).

2. Results and discussion

2.1. Biomedical adhesive polymer synthesis and characterization

In order to synthesize poly(AMPS-*co*-MDOPA), first, the monomer *N*-methacryloyl-3,4-dihydroxyl-L-phenyl-alanine (MDOPA) was synthesized as previously reported.[5,27] Briefly, levodopa (L-DOPA) was methacrylated utilizing methacryloyl chloride with sodium tetraborate decahydrate (borax) to protect the hydroxyl groups of the catechol during the reaction. The synthesized vinyl monomer, MDOPA (Fig. S1, ESI†), was then able to be copolymerized with AMPS. The copolymer was prepared through thermally initiated radical polymerization without the addition of any crosslinkers, as shown in Fig. 1b. The effect of the ratio of MDOPA to other monomers of copolymer adhesives has been previously reported and considered.[50,51] In this study, we utilized a reaction molar ratio of 85 : 15 of AMPS to MDOPA to obtain strong adhesion properties for application on the skin, while maintaining the beneficial hydrophilicity and biocompatibility properties provided by AMPS.

The synthesized poly(AMPS-*co*-MDOPA) was purified by dialysis. During the dialysis, it was important to consider the acidity of the sulfonic acid portion of the AMPS repeating unit due to the sulfonic acid moiety as this may lead to the prepared

adhesive remaining too acidic for the desired biocompatibility. Considering this, dialysis was performed in a PBS (phosphate buffered saline) solution (pH 7.4) rather than DI water to neutralize the sulfonic acid moiety of the polymer, which will improve the biocompatibility. The neutralization of the polymer is also directly relevant to AMPS drug loading capabilities as they are most effective at a neutral pH.[39] When the purification was concluded, the polymer was then lyophilized to yield a light pink powder (yield 77%, Fig. 1c). This reaction was scaled up to 10 grams without yielding sacrifices or property changes. The polymer powder demonstrates no inherent adhesive properties when dried, however, if exposed to even a small amount of water, it swells into a highly viscous gel-like liquid. This can then be applied to a targeted area using a syringe or a pipette.

To confirm the chemical structure of poly(AMPS-*co*-MDOPA), ^{1}H NMR spectroscopy was performed. In small concentrations, the adhesive can be readily dissolved in D_2O, making it the ideal solvent for NMR due to its poor solubility in most organic solvents. The most identifiable moieties for determination of the copolymer ratio are the three hydrogens associated with MDOPA in the benzene ring of the catechol group (broad peak at 6.79 ppm, Fig. 1d), as well as the peak associated with the two hydrogens closest to the sulfonic acid group in AMPS repeating units (broad peak at 3.30 ppm, Fig. 1d). The integration demonstrates the successful copolymerization of AMPS and MDOPA. The NMR structure in Fig. 1d shows the high purity of the copolymer following purification. After polymerization, the repeating unit ratio between the monomers was found to be almost identical to the theoretical ratio (input ratio of monomers, 85 : 15). The resulting repeating unit ratio was 88 : 12 AMPS to MDOPA found from the integration of peaks in the ^{1}H NMR spectrum. The integration of all peaks and their assignments is provided in the ESI† (Fig. S2). The primary peaks used to determine the copolymer's repeating unit ratio were the catechol hydrogens of the MDOPA unit (g, 6.5–6.9 ppm) and the amide hydrogen of the AMPS (a, 7.2–7.9 ppm). Since the broad peak at 7.2–7.9 ppm includes contribution from both *a* (amide in AMPS) and *d* (amide in MDOPA), the integration of *d* (amide in MDOPA) was subtracted from the overall integration at 7.2–7.9 ppm in Fig. 1d. The 88 : 12 ratio between AMPS and the MDOPA unit was consistent through several individual copolymer adhesive synthesis batches. Due to the poor solubility of the polymers in common gel permeation chromatography (GPC) solvents (THF and DMF) and their strong adhesion to the GPC column packing materials in aqueous GPC, molecular weight determination by GPC could not be performed.

2.2. Bulk adhesion properties: lap shear strength test

The bulk adhesion properties (maximum adhesion strength and work of adhesion) were determined and quantified utilizing a lap shear strength test and probe tack test on different substrates. For the lap shear strength test, the substrate chosen was PET (Mylar®) films. Dry PET films were utilized as an additional adhesion test to that of the wet adhesion probe tack test, as it allows uniform data that we can compare with other adhesives of similar adhesive strength that lack wet adhesion properties. In addition, the PET film works as a good baseline for adhesion lap shear strength testing due to PET's excellent tensile strength and flexibility.

The test was performed through repetition of the same method for all trials done. For each test, 30 mg of adhesive was applied to an area of 2.0 cm × 2.0 cm of the PET film. For poly(AMPS-*co*-MDOPA), the adhesive powders were first swollen with 40 μL of DI water for 2 hours as shown in Fig. 2c. The overlapping films were then placed underneath a 100 g weight for varying times to determine the setting time and the related strength of the adhesive. While most pressure sensitive adhesives have much greater adhesion strength when applying pressure for long periods of time, due to the biomedical applications this adhesive is designed for, short pressure application times were chosen for testing the clinically realistic adhesion strength. Once the desired time had passed, the weight was removed and the PET films were transferred to a Shimadzu tensile-compression tester and tightly secured, followed by pulling until failure (Fig. 2e). The resulting force *versus* displacement curve could then be utilized to determine adhesion strength and the work of adhesion for each sample.

An adhesive's strength is reliant on the time during which pressure is applied to the adherends, also known as the setting or tack time.[52] The tack time has a major impact on biomedical adhesives, as applying pressure to the site for a long time may be difficult, painful, or damaging to the area. However, while short times, or ''instant'' adhesives, are extremely important, there are few papers factoring the tack time as a crucial factor.[32,53,54] In clinical applications, biomedical adhesives that are applied during or following surgery requiring a long period of time in which pressure must be applied for the adhesive to set to the skin is not reasonable, and as such, an adhesive with strong adhesion strength with a short setting time is very important. Our adhesive was tested at a maximum of 1 hour to show its adhesion strength after application for a long time, but the focus was on short setting times of 30 seconds, 2 minutes, and 5 minutes (Fig. 2a–c).

Separately, the AMPS monomer was homo-polymerized through the same method as the copolymer synthesis for the comparative test. The homopolymer poly(AMPS) can demonstrate the adhesion strength benefits provided by the addition of the catechol moiety to the copolymer. In addition to the homo-poly(AMPS), poly(AMPS-*co*-MDOPA) was compared with another commercial adhesive, a conventional Elmer's glue stick. The rationale for this demonstration is to show similar work of adhesion of a soft adhesive to that of our biomedical adhesive, while demonstrating the superior adhesion strength that the addition of catechol provides as well.

For the 30 s setting time, the adhesion strength of poly(AMPS-*co*-MDOPA) was 2.8 kPa, while the adhesion strength for poly(AMPS) and the glue stick were 0.1 kPa and 1.5 kPa respectively (Fig. 2a and b). The difference in them greatly increases as the setting is increased to 2 minutes, as adhesion strength becomes 4.3 kPa for our copolymer, and 0.1 kPa and 1.9 kPa for the poly(AMPS) and the glue stick.

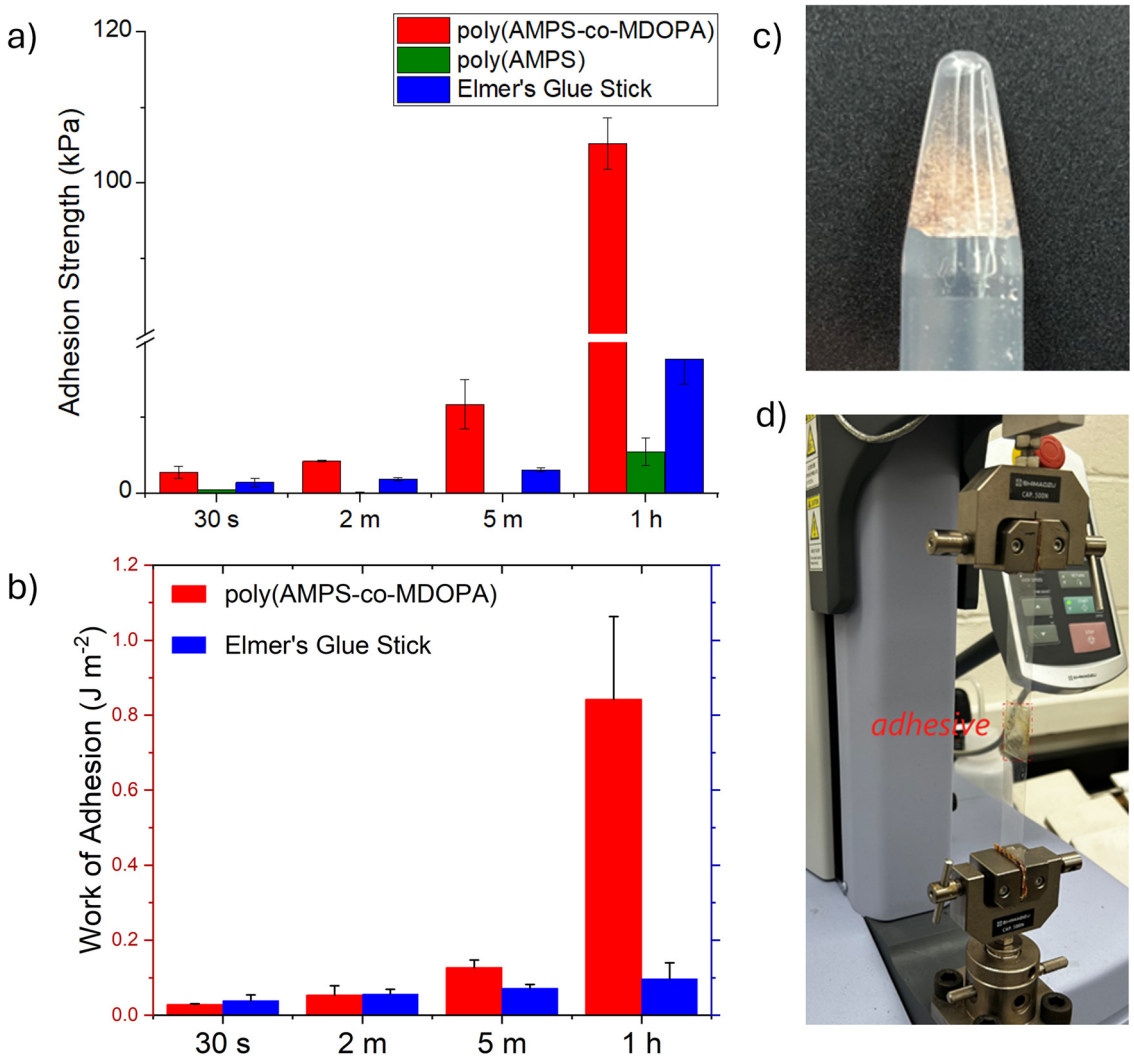

Fig. 2 Lap shear strength tests performed at various setting times demonstrating the (a) adhesion strength comparison between poly(AMPS-*co*-MDOPA), poly(AMPS), and a commercial Elmer's glue stick, (b) work of adhesion comparison between poly(AMPS-*co*-MDOPA) and a commercial Elmer's glue stick, (c) swollen polymer used for adhesion testing and (d) dry PET film adhesion testing setup utilizing a Shimadzu tensile tester.

This demonstrates that an addition of a minute and a half leads to a 68% increase in adhesion strength for our copolymer, while only 13% and 28% increases for poly(AMPS) and the glue stick. This trend continues after 5 minutes, in which the copolymer adhesion strength increases to 11.8 kPa, while the poly(AMPS) and glue stick exhibit 0.5 and 3.1 kPa adhesion strengths respectively. This increase from the 30 s initial condition is an increase of 320% for the copolymer, while the poly(AMPS) and the glue stick exhibit adhesion strengths of 300% and 110% respectively. If left for a much longer period, we can see the percentage difference increases dramatically for our copolymer, leading to a 3630% increase in adhesion strength (105 kPa), however, the poly(AMPS) and glue stick experience much higher adhesion strength increases of 4510% (5.5 kPa) and 1090% (17.8 kPa). This high increase is important, as conventional adhesives usually require much higher setting times than a few minutes. These results demonstrate our adhesive's ability to reach higher adhesion strengths at a faster rate, a quality that is ideal for a biomedical adhesive that requires quick application time without prolonged pressure to adhere.

The fast-setting time (*i.e.*, instant adhesion) is likely due to the electrostatic interactions from the ionic charges present in the AMPS repeating units' sulfonic acids of the copolymer with the ammonium ions present on the surface of the skin (Fig. 1a). While the strong adhesion strength from the catechol group can be shown in the 1 hour of setting time, electrostatic interactions can occur nearly instantly upon contact, enabling initial adhesion within very small-time frames. The strong adhesion strength is primarily due to covalent bonding between the adhesive and substrate (Fig. 1a), as the covalent bond strength is high, however, the covalent bond formation takes time. Thus, electrostatic interactions on the surface of the skin (Fig. 1a) are highly advantageous due to their fast initial adhesion formation.

As shown in Fig. 2b, the work of adhesion (J m^{-2}) of an adhesive is a measure of the work needed to fully separate the

adhesive from the substrate. This can also be considered the biomedical adhesive's toughness. Due to the substantially weak adhesion properties of poly(AMPS) compared to other adhesives, as shown in Fig. 2a, the work of adhesion comparison between poly(AMPS-*co*-MDOPA) and the glue stick is described in Fig. 2b. At the 30 s of setting time, the copolymer had a work of adhesion of 0.03 J m^{-2} and the glue stick had a work of adhesion of 0.04 J m^{-2}. Despite the similar work of adhesions, our copolymer exhibited a much higher adhesion strength (2.8 kPa) than the glue sticks at a short setting time as discussed above (Fig. 2a). In other words, poly(AMPS-*co*-MDOPA) is not as ductile as the glue stick at the 30 s of setting time. As shown in Fig. 2b, the difference in the work of adhesion between the copolymer adhesive and the glue stick becomes smaller as the setting time increases to two minutes, with the copolymer reaching 0.05 J m^{-2} (an 87% increase) and the glue stick reaching 0.06 J m^{-2} (a 45% increase). The copolymer's toughness increases significantly from the two-minute setting time at a setting time of 5 minutes to 0.13 J m^{-2} (340% increase) while the glue stick exhibits a work of adhesion of 0.07 J m^{-2} (85% increase). The one-hour time point clearly shows the influence that setting time has on the toughness of the copolymer adhesive, since the glue stick only exhibits a work of adhesion of 0.1 J m^{-2} after 1 hour (150% increase), while the adhesive copolymer's work of adhesion increases to 0.842 J m^{-2} (2840% increase). This indicates that while the work of adhesion of the adhesive is quite low at short setting times, increasing the setting time has tremendous results on this measurement. This allows for high tunability in the adhesion properties by determining the setting time of the adhesive that yields the ideal work of adhesion and adhesion strength.

2.3. Bulk adhesion properties: porcine skin probe tack test

To determine the biomedical wet adhesive properties of the reported copolymer, a wet probe tack test was performed with a porcine skin substrate. To perform this experiment, two identical pieces of porcine skin were cut to a 3 cm diameter circle and prepared for adhesion testing. The detailed sample preparation method is described in the Experimental section. The dry adhesive copolymer powder (100 mg) was added to the wet porcine skin to perform adhesion testing. The actual test setup is shown in Fig. 3a and b. The probe tack test applied a preload force of 1 N before starting the adhesion test. The probe was then pulled apart at a crosshead speed of 1 mm min^{-1} until the adhesion failed (disconnection). The test yielded force (N) *versus* displacement (cm) curves (Fig. S3, ESI†), and this data was used to derive the results shown in Fig. 3c. The primary reason for performing a probe tact test rather than an additional lap shear strength test is that the wet adhesion test was technically challenging to perform using a lap shear test. When the test samples were set up, the moisture would run down the porcine skin sample, causing it to yield inconsistent results, and the heavy weight of the water-swollen porcine skin made it very flexible and heavy, making it difficult to perform the vertical test due to the sample moving outside of the force applied from the tensile tester.

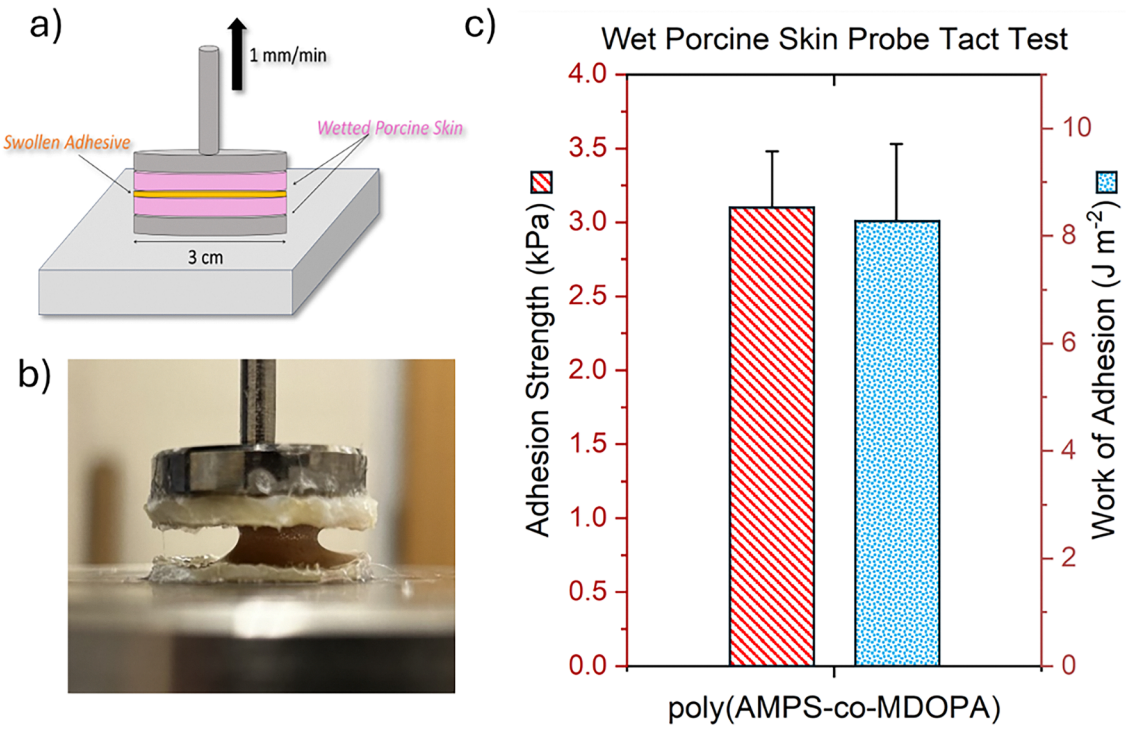

Fig. 3 (a) Illustration of probe tack test experiments, (b) photograph of poly(AMPS-*co*-MDOPA) probe tack testing on porcine skin and (c) poly(AMPS-*co*-MDOPA)'s adhesion strength and work of adhesion on porcine skin.

Previous studies have shown that porcine skin is topologically and biologically very similar to that of human skin, making it an excellent model for the determination of the wet skin adhesion properties of human skin.[14,55,56] In addition, to ensure the porcine skin surface properties were similar to that of human skin, we investigated the humidity and oil content of the porcine skin prior to testing using a two probed skin moisture analyzer to yield an average humidity of 47% with 24% oil detected. This lines up very well with values determined through the same analysis on the human skin done with the same analyzer (averages of 41% and 27% respectively tested over 5 different individual forearms), indicating that our porcine adhesion studies should be easily replicable in human skin subjects.

When the DOPA moiety is added to AMPS to create our new copolymer, poly(AMPS-*co*-MDOPA), it showed significantly stronger adhesion strength averaging 3.10 kPa (Fig. 3c) when compared to the homopolymer, which showed no wet adhesion properties. An increase in the amount of MDOPA to the copolymer would increase the copolymer adhesion strength, however, excessive addition of MDOPA segments into the copolymer leads to a reduction in hydrophilicity, as MDOPA possesses lower hydrophilicity compared to AMPS due to its lack of ionic attraction to water.

In general, an optimized amount of crosslinkers can be employed in adhesive polymers to increase adhesion,[27] however, too much crosslinking may lead to gelation, thereby increasing rigidity of the adhesives, leading to a harder adhesive more prone to poor wetting (intimate contact of adhesive and spread over a given substrate) on the substrate surface. For the developed poly(AMPS-*co*-MDOPA), additional chemical crosslinking is not necessary due to physical crosslinking that can occur through hydrogen bonding between the catechol and the sulfonic acid moieties within the copolymer matrix.[57]

The type of failure that occurs for an adhesive can provide a significant amount of information regarding its properties. If all the adhesive is located on one of the two adherends with poor regularity, it is adhesion failure, and if the adhesive is located on both adherends regularly, it is cohesive failure. The copolymer, poly(AMPS-*co*-MDOPA), demonstrated adhesive failure rather than cohesive, indicating the strong adhesion to the surface was likely limited by the wetness of the skin. However, the tests on dry PET film substrates showed cohesive failure, with the same amount of adhesive remaining on both attached substrates.

The adhesion strength for this copolymer is comparable with other reported values for similar biomedical adhesives such as fibrin glue (10^3–10^4 Pa), though the difference in skin used, moisture levels, and amount of adhesive used per surface area can affect these values greatly.[11,58] In addition, the work of adhesion of the copolymer is within a similar range to other biomedical adhesives. Fig. 3c shows that the work of adhesion is 8.24 J m^{-2}, a value that indicates a very flexible adhesive, in which the maximum adhesion strength (kPa) is comparable to other adhesives, and a large amount of work of adhesion (J m^{-2}) is still necessary to fully separate the two surfaces, indicating soft and tough adhesion properties of the copolymer adhesive.

2.4. Biocompatibility and cytotoxicity assays

Any biopolymer adhesive being developed for topical drug delivery would need to be first tested for potential cytotoxic effects. To achieve this, we used primary dermal fibroblasts obtained from human skin as described previously.[59] To mimic the outer layer of terminally differentiated and non-dividing cells on human skin, we used growth arrested, non-dividing dermal fibroblasts and exposed them to increasing concentrations of our adhesive. After 48 hours, cells were stained with the live-cell permeable nuclear dye Hoechst 33342 to color the nuclei of all cells blue, while the live-cell impermeable nucleic acid dye propidium iodide was used to stain any dead cells red. Cells were then imaged by fluorescence microscopy. Hydrogen peroxide (H_2O_2) treatment was used as a positive control for cell death in Fig. 4, 5 and Fig. S11–S13 (ESI†). To evaluate both acute and cumulative effects of the polymer on cells, we then conducted cytotoxicity tests over two time periods, a short 48-hour test, and a longer 6-day test. Brightfield images were collected and merged with the blue and red channels to obtain the overlay images shown on the bottom panels.

In Fig. 4a, treatment of non-dividing human dermal fibroblasts with up to 10 mg mL^{-1} concentrations of the polymer results in very low numbers of dead cells, similar to the untreated cells, based on the near complete absence of cells with red staining. However, cell death indicated by red staining was readily observed upon treatment of the cells with 12.5 mg mL^{-1} of the polymer. We further confirmed these data using the more sensitive method of flow cytometry to quantify the percentage of dead cells following exposure to the adhesive (Fig. 4b). The flow cytometry plot shows a multicolored ''heat map'', with blue color indicating ''cold'' or few cells, green to yellow indicating ''warm'' or moderate numbers of cells, and red indicating ''hot'' or high numbers of cells (Fig. S4 in the ESI†). The plot comprises of clusters of dots, with each dot representing an individual cell whose position on the plot is determined by the amount of red and blue signal present in the cell. The *X*-axis denotes increasing blue signals, while the *Y*-axis denotes increasing red signals. Note that all cells carry similar amounts of blue signal due to the presence of similar amounts of DNA in each cell, while the dying cells also carry moderate amounts of red signal, with the dead cells having the highest amounts of red signal. Since the vast majority of cells in the sample are alive, due to their similar levels of blue signal and absence of red signal, they give rise to the hot red cluster on the bottom right of the plot. On the other hand, the dead cells with both blue signal as well as high amounts of red signal show up in the demarcated area in the upper right of the plot (while cells in the process of dying with intermediate levels of red signal will show up below that). The 10 mg mL^{-1} polymer concentration results in cell death at levels similar to naturally occurring cell death among untreated cells in this experiment, while the 12.5 mg mL^{-1} polymer concentration results in a 3-fold higher level of cell death compared to the untreated cells.

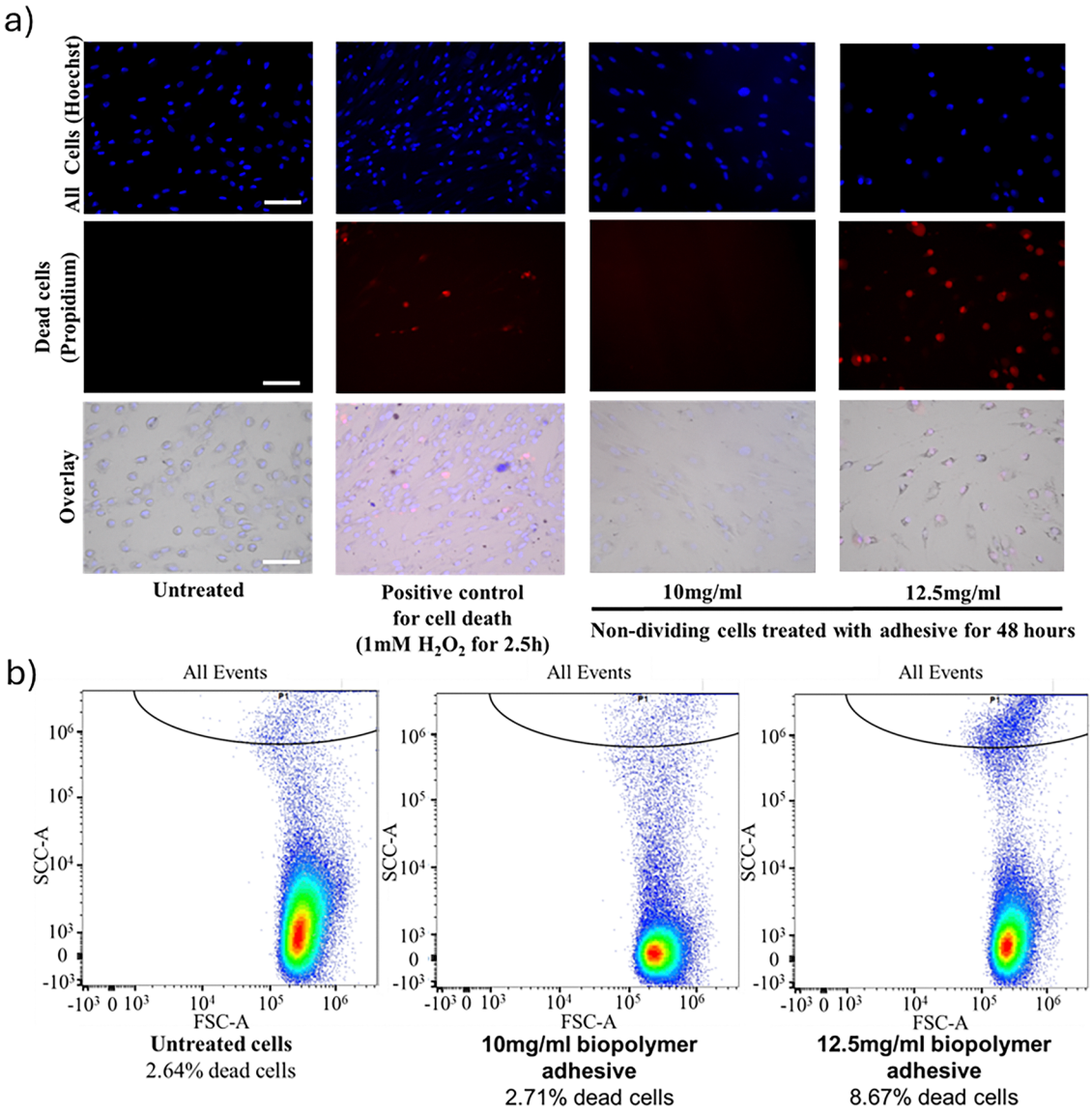

Fig. 4 (a) Effect of direct poly(AMPS-*co*-MDOPA) addition to non-dividing human dermal fibroblasts. No appreciable cell death is observed below polymer concentrations of up to 10 mg mL^{-1} following 48 hours exposure. (b) Quantification of cell death in some of the samples shown in panel A by flow cytometry. The *X*-axis represents the intensity of the blue signal, while the *Y*-axis represents the intensity of the red signal. A clear increase in the dead cell population is observed in the upper right corner of the flow cytometry plot upon exposure to 12.5 mg mL^{-1} of the polymer for 48 hours.

Overall, these data show that non-dividing primary human dermal fibroblasts were not sensitive to poly(AMPS-*co*-MDOPA) at concentrations below 10 mg mL^{-1} following 48 h exposure (Fig. 4a).

Since the actively dividing (proliferating) cells present in the inner layers of the skin can have a different threshold for cytotoxicity especially while undergoing DNA replication during S phase when cells are most vulnerable to perturbations, we also exposed proliferating primary human dermal fibroblasts to different concentrations of the adhesive. Proliferating cells did exhibit a slight increase in sensitivity to the adhesive polymer yet showed no appreciable sensitivity to it at concentrations below 8 mg mL^{-1} after 48 hours of exposure (Fig. S5, ESI†). We also tested for cytotoxic effects upon longer exposure of the cycling cells to the adhesive and found no cytotoxicity below 5 mg mL^{-1} even after 6 days of exposure to the adhesive polymer (Fig. S6, ESI†). From these experiments, we conclude that the adhesive polymer is not cytotoxic at concentrations below 5 mg mL^{-1} even upon extended exposure of dividing cells *in vitro*.

2.5. Comparison of the toxicity of the biopolymer adhesive with existing topical dermatological treatments

The *in vitro* experiments involving the direct exposure of dividing cells to the adhesive is a very different situation than the *in vivo* application of the adhesive to live human skin with its multiple layers of protective barriers. Hence, our *in vitro* experiments shown in Fig. 4 are likely to be exaggerating the actual

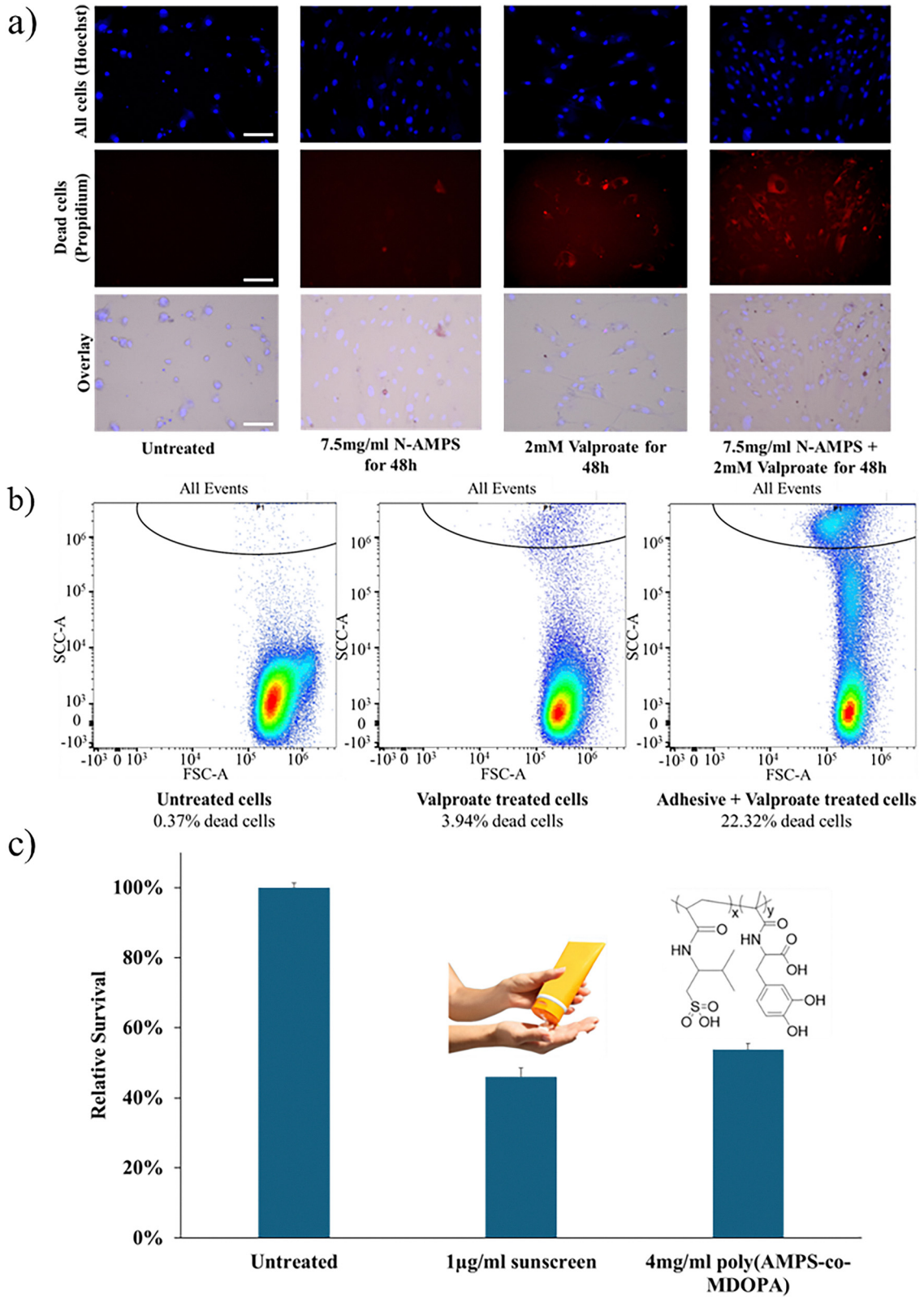

Fig. 5 (a) Effect of valproate delivery to human dermal fibroblasts with and without the poly(AMPS-*co*-MDOPA). Some cell death is observed in fibroblasts treated with valproate alone, but the delivery of the valproate through the biopolymer adhesive was highly synergistic and strongly amplified the cytotoxic effect. (b) Quantification of cell death shown in panel a by flow cytometry. (c) Comparison of the survival of proliferating human dermal fibroblasts following a 7-day direct exposure to a low dose (1 µg mL^{-1}) of a commercial sunscreen that is approved for use on human skin, and 4 mg mL^{-1} of poly(AMPS-*co*-MDOPA).

cytotoxicity of the adhesive and it is very likely to be safe and well tolerated on live skin. To directly test if this was likely to be the case, we compared the effects of a small amount (1 μg mL^{-1}) of a popular commercial sunscreen approved for use on human skin to a much higher amount (4 mg mL^{-1}) of our biopolymer adhesive on cultured human dermal fibroblasts following a 7-day exposure (Fig. 5c). The polymer concentration used in this experiment (4 mg mL^{-1}) was 4000 times higher than the sunscreen concentration (1 μg mL^{-1}), yet both resulted in comparable levels of cell death. Therefore, the polymer exhibits approximately 4000-fold lower toxicity when directly applied to cultured skin fibroblasts compared to the commercial sunscreen. This highlights the high likelihood of our biopolymer adhesive being safe for use on intact human skin, given its relatively low toxicity on isolated skin cells compared to currently existing dermatological treatments. These *in vitro* test results would need to be formally confirmed through testing on animal models in future studies.

2.6. Drug delivery using the biopolymer adhesive

Valproate, a histone deacetylase (HDAC) inhibitor, triggers apoptosis in cells[60] and exhibits antifibrotic effects,[61] suggesting its potential use to treat fibrotic skin disorders such as keloids. In the new copolymer poly(AMPS-*co*-MDOPA), the hydrogen bonding from the amide group endows AMPS containing polymer to serve as a drug delivery vehicle, as the hydrogen bonding stably holds drugs such as the carboxylate containing valproate (Fig. S7, ESI†).[37,39,41] This hydrogen bonding between the drug and adhesive copolymer will enable the stable storage of drug in the biomedical adhesive copolymer matrix as shown in Fig. S7 (ESI†). Then, the loaded drug can be released to a target area by passive diffusion over an extended period following application.

Given that our adhesive poly(AMPS-*co*-MDOPA) is non-toxic to cells *in vitro* at concentrations below 8 mg mL^{-1} within 48 hours of exposure (Fig. S5, ESI†), next we tested the effect of the drug valproate on the cells exposed to the drug either directly or following incorporation of the drug into the adhesive. Exposure of proliferating primary human dermal fibroblasts to 2 mM valproate alone resulted in the predicted cytotoxicity within 48 hours (Fig. 5a). The detailed rationale for the use of proliferating primary human dermal fibroblasts is provided in the Experimental section. In this study, tests using proliferating primary human dermal fibroblasts were conducted to evaluate the effects of valproate and poly(AMPS-*co*-MDOPA) for potential keloid treatment in the future. It is important to note that the cellbased assays shown in Fig. 5 were performed using normal (non-keloidal) cells as a preliminary study, serving as a foundation for future research involving keloid-specific models, with a primary focus on biological and pharmaceutical science. As shown in Fig. 5, the test results indicate that when sodium valproate (2 mM) was combined with the adhesive (7.5 mg mL^{-1}), the cytotoxicity was significantly enhanced in a synergistic manner, an effect not attributable to the adhesive alone. This effect was also observed using flow cytometry, which suggests a 5–6-fold higher cytotoxicity (Fig. 5b). Although the underlying mechanism for this observed increase in cytotoxicity is unclear at present, it may be a desirable effect in certain therapeutic modalities where the end goal is to kill cells within the diseased skin tissue *via* local topical application. The cell tests shown in Fig. 5 were conducted using normal (non-keloidal) cells as an initial study, providing a basis for future research focused on keloid-specific cell and animal models, with an emphasis on biological and pharmaceutical research themes. Unlike cancer cells, keloid cells are not immortal and share many similarities with normal cells, making them challenging to treat using conventional treatment methods, as they cannot be easily distinguished from normal cells. A key advantage of our treatment approach using a HDAC inhibitor containing poly (AMPS-*co*-MDOPA) is its targeted application to just the affected skin areas, which would help minimize potential side effects on surrounding healthy tissues.

3. Conclusion

The novel biomedical adhesive, poly(AMPS-*co*-MDOPA), was synthesized combining the advantageous properties of the catechol containing the MDOPA monomer for mussel-inspired adhesion and the AMPS monomer for hydrophilicity and electrostatic interaction-originated adhesion. The thermally initiated free radical polymerization of the two vinyl monomers led to a new biomedical adhesive with excellent fast-acting adhesion properties comparable to modern biomedical adhesives such as fibrin glue. To determine the adhesion strength (kPa) and work of adhesion (J m^{-2}), two types of adhesion tests, lap shear test and probe tack test, were performed. The adhesion tests varied the setting time, and proved the fast adhesion and strong adhesion properties which are essential for biomedical adhesives, particular for topical applications on the skin. Cytotoxicity testing also proved the excellent biocompatibility of our copolymer adhesive in the presence of primary human dermal fibroblasts. Given that mammalian skin has multiple protective features, we believe that the cytotoxic effects observed at higher concentrations of our biomedical adhesive are exaggerated in our *in vitro* assays, and that our biomedical adhesive will be very well tolerated by mammalian skin. Hence, our future endeavors with this new biomedical adhesive would be initially aimed at testing its performance on live animal skin, with the eventual goal of utilizing the drug delivery capabilities inherent in the system to deliver drugs for dermatological conditions. This would include the delivery of drugs such as HDAC inhibitors and other drugs to the wound site of keloids in humans following their surgical excision to act as not only as a drug delivery agent for drugs that block keloid recurrence, but also a soft biomedical adhesive to cover the wound site and allow healing to occur.

4. Experimental

4.1. Materials

All reagents were purchased from Sigma-Aldrich Co. and TCI America and used without further purification unless otherwise

stated. MDOPA was synthesized and characterized as previously reported in the literature.[4,5,62] Porcine skin was purchased from a local sausage manufacturing facility. Florida State University Animal Care and Use Committee (ACUC) protocols were not considered because there were no procedures involving live animals.

4.2. Synthesis of poly(AMPS-*co*-MDOPA)

MDOPA (1.88 g, 7.12 mmol, 0.15 equiv.), AMPS (8.4 g, 40.53 mmol. 0.15 equiv.), and 2,2′-azobis(2-methylpropionitrile (radical initiator, 0.24 g, 0.71 mmol, 0.03 equiv.) were mixed in DI water/1,4 dioxane co-solvent (75 mL; the volume ratio of solvents was 1 : 1). The mixture was degassed for 15 min by using dry nitrogen gas and then stirred for 16 h at 65 °C, giving rise to the copolymer. Following polymerization, the reaction solution was cooled to room temperature, then it was transferred to a regenerated cellulose membrane (MWCO: 1 kD, Spectra/Por) to remove small molecular size impurities through dialysis. The dialysis was performed in a PBS solution in DI water for 48 h while being stirred at low speeds. The PBS solution was changed every 2 hours for the first 8 hours, then every 8 hours following. Once dialysis was completed, the copolymer was lyophilized to remove water, in a Labconco freeze dryer at −48 °C and 1 mbar yielding a dry flake-like powder with a slight pink color (7.242 g, 70.45% yield). The chemical structure was analyzed by ^{1}H NMR (600 MHz, D_2O) spectroscopy. Molecular weight analysis of polymers using gel permeation chromatography (GPC) could not be conducted because poly(AMPS-*co*-MDOPA) was not soluble in organic solvents (DMF and THF) for GPC. Aqueous GPC could not be used because the catechol groups in the adhesive copolymer may form permanent bonds with the packing materials in the GPC column.

4.3. *In vitro* cytotoxicity cell experiments

4.3.1. Cell culture. Primary human dermal fibroblast cells at low passage were cultured in Dulbecco's Modified Eagle's Medium (DMEM) supplemented with 10% fetal bovine serum (FBS) and 1% penicillin–streptomycin and 1× Primocin antimicrobial cocktail (Invivogen) as described previously.[59] Cultures were maintained at 37 °C in a humidified atmosphere containing 5% CO_2.

"Primary" cells are obtained directly from patients' tissues and retain most of their *in vivo* properties, including a finite number of cell divisions (usually about 15 divisions or so for these cells) that they can undergo before dying off (*i.e.*, undergoing senescence). This contrasts with the "cell lines" that are used in most research, and these are either spontaneously or artificially immortalized versions of the primary cells and will keep on dividing forever, like cancer cells. Although useful for research, the immortalized cells are less like the original cells obtained from the patient tissues *in vivo*, especially with regards to their replicative potential.

"Proliferating" cells are actively growing and dividing and undergoing DNA replication. Cells undergoing DNA replication during S phase are at their most vulnerable to any external stress and so proliferating cells are much more sensitive for detecting cytotoxic effects caused by treatment with any external agent (non-dividing or "quiescent" cells are less sensitive). Our tests were designed to assess the sensitivity of both proliferating and non-dividing cells (also known as growth-arrested, density-arrested, contact-inhibited cells).

4.3.2. Polymer solution preparation. A stock solution of the adhesive, poly(AMPS-*co*-MDOPA), was prepared in the cell culture medium at 200 mg mL^{-1} from which various concentrations used in our experiments were directly diluted in cell culture media in each well.

4.3.3. Microscopy based qualitative cytotoxicity assay. Primary dermal fibroblast cells were seeded into 24 well plates at a 10% confluency for experiments using cycling cells and at 50% confluency for experiments using contact inhibited growth arrested cells. To assess the effects of the adhesive, poly(AMPS-*co*-MDOPA), on different growth states, cells were used at 25% confluency (cycling cells) or at 100% confluency (growth-arrested non-dividing cells). Cell cultures were exposed to different concentrations of the adhesive for different periods of time as indicated in the figure legends. To evaluate the drug delivery ability of the adhesive, exponentially grown primary human dermal fibroblast cultures at 25% confluency were treated for 48 hours either directly with 2 mM sodium valproate, or with a 7.5 mg mL^{-1} adhesive solution containing the valproate. Hydrogen peroxide (H_2O_2) treatment was used as a positive control for cell death because of oxidative stress. Cytotoxicity was assessed using fluorescence microscopy. Post-treatment, cells were dual stained with the live cell permeable nuclear dye Hoechst 33342 at 1 μg mL^{-1} to color all cell nuclei blue, and the live cell impermeable nucleic acid stain propidium iodide at 1 μg mL^{-1} to color dead cells red. The cells were stained for 30 minutes at 37 °C in the cell culture incubator. Fluorescence images were captured using a fluorescence microscope (Keyence BZ-X810; Keyence of America, Itasca, IL) equipped with blue and red filters. Bright field imaging was also performed, and the three channels were overlaid to provide the composite representative images shown in the figures. The images provide a qualitative representation of cell viability, with the nuclei of all the cells appearing only blue, while the dead cells are dual stained with red and blue.

4.3.4. Flow cytometry based quantitative cytotoxicity assay. Dermal fibroblasts exposed to different concentrations of the adhesive, poly(AMPS-*co*-MDOPA), valproate or H_2O_2 for different times were stained with Hoechst 33342 at 1 μg mL^{-1} and propidium iodide at 1 μg mL^{-1} for 30 minutes at 37 °C in the cell culture incubator. Cells were then washed three times with phosphate buffered saline (PBS) to remove unincorporated stains, following which the cells were dissociated with trypsin. The dissociated cells were recovered by centrifugation, washed with PBS and fixed in ice cold 70% ethanol and stored at 4 °C until analysis. Prior to flow cytometry analysis, cells were recovered by centrifugation and resuspended in PBS. Sample were analyzed on a Becton-Dickinson FACSAria flow cytometer.

4.3.5. Cell counting based quantitative cytotoxicity assay. Primary dermal fibroblast cells were seeded into 24 well plates at 10% confluency. After the cells had attached, they were

treated in triplicate with the indicated concentrations of the different agents described, or the adhesive biopolymer for 7 days. Viable cells were dissociated using trypsin and counted on a Coulter Counter to determine the percentage of surviving cells following the different treatments by comparing them to the survival of untreated cells.

4.4. Tensile adhesion testing (lap shear strength test)

Determination of the dry adhesion strength of the copolymer with non-skin substrates was evaluated using a Shimadzu EZ-LX Universal tensile tester. The maximum adhesion strength and work of adhesion of our copolymer (in comparison with a traditional glue stick) on these Mylar® (PET) films was determined by utilizing a lap shear strength test. Two Mylar® films of length 5.0 cm × 2.0 cm were used, and the adhesive was applied to a 2.0 cm × 2.0 cm overlapping area. The overlapped PET film was placed underneath 100 g weights for varying times, before being moved to the tensile tester. Strips were then pulled apart to failure at a crosshead speed of 1 mm min^{-1}. The collected force *versus* displacement curve was analyzed to determine adhesion strength by dividing the maximum force by the overlapping area. The work of adhesion, expressed in J m^{-2}, was calculated by dividing the adhesion energy, obtained from the integral of the force *versus* displacement curve, by the contact area in m^2. The test was repeated at least 5 times for each condition to obtain averages as well as the standard error of the mean. The adhesion strength, with the SI unit of Pa, is calculated by dividing the maximum force by the overlapping adhesion area. The work of adhesion, with the SI unit of J m^{-2}, is calculated by integrating the force *versus* displacement curve and then dividing by the adhesive overlap area. All PET films were laser cut to ensure the dimensions were identical in all experiments. All lap shear strength tests were carried out 3 times each to ensure consistency, and reported in Fig. 2 as the standard error of the mean.

4.5. Porcine skin probe tack test

To determine the maximum adhesion strength of the adhesive on porcine skin, a probe tack test was conducted. The results were obtained by utilizing a Shimadzu EZ-LX Universal tensile tester. To perform the tests, the porcine skins were wet with DI water prior to adhesive application. The porcine skin was then cut into circles with a diameter of 3 cm. These porcine skin pieces were placed in a hexane/ethanol 1 : 1 mixture overnight to remove fat and oil from the surface of the skin. Following this, the porcine skins were wetted by first placing the skins in DI water and then left to sit in it for five minutes. The porcine skin was then removed and adhered to either ends of the tensile probes to begin the experiment. The bottom side of the porcine skin was dried, then the porcine skin samples were superglued to the metal plates using ample amounts of glue to ensure a strong hold. Then, 100 mg dry copolymer powder was applied to the surface of the wet porcine tissue. The adhesive was allowed to swell for 5 minutes before an adhesion test was done. The tissue samples were held together under 1 N of force (~100 g weight). The porcine samples were then pulled apart at a crosshead speed of 1 mm min^{-1} and pulled to failure. The maximum adhesion strength was determined by taking the obtained force (N) *vs.* displacement (cm) curves and dividing force by the overlapping area ($A = \pi r^2$) in meters to obtain the stress in Pa. Work of adhesion was derived utilizing the same data by integrating the force *vs.* displacement curve and dividing it by the overlapping area to give the work of adhesion (J m^{-2}). The integration of these curves was done in MATLAB by utilizing the trapz function. The test was repeated at least 15 times to get averages as well as the standard error of the mean.

4.6. Characterization

Nuclear magnetic resonance (NMR) spectra of the samples were obtained by using a Bruker Avance III 600 MHz NMR spectrometer. NMR was performed by taking 10 mg of polymer in 0.7 mL of D_2O. Adhesion properties (maximum adhesion strength and work of adhesion) of the samples were assessed using a Shimadzu tensile-compression tester (Model: EZ-LX) equipped with a 200 N force transducer (Interface Ltd model: SM-200 N-168).

Data availability

The experimental data supporting the findings of this study, including characterization data for all synthesized compounds, are provided in the figures, tables, ESI,† and the Experimental section of this article. Additional details, such as more detailed experimental procedures, optimized reaction conditions, and data not discussed in the article, are available from the corresponding author upon reasonable request.

Conflicts of interest

There are no conflicts to declare.

Acknowledgements

This work was funded by the Creative Collision at Florida State University initiative.

References

1 F. Scognamiglio, A. Travan, I. Rustighi, P. Tarchi, S. Palmisano, E. Marsich, M. Borgogna, I. Donati, N. De Manzini and S. Paoletti, *J. Biomed. Mater. Res. B Appl. Biomater.*, 2016, **104**, 626–639.
2 S. Burks and W. Spotnitz, *AORN J.*, 2014, **100**, 160–176.
3 J. Saiz-Poseu, J. Mancebo-Aracil, F. Nador, F. Busqué and D. Ruiz-Molina, *Angew. Chem., Int. Ed.*, 2019, **58**, 696–714.
4 I. Pramudya, C. G. Rico, C. Lee and H. Chung, *Biomacromolecules*, 2016, **17**, 3853–3861.
5 M. Kim and H. Chung, *Polym. Chem.*, 2017, **8**, 6300–6308.
6 K. Han, Q. Bai, W. Wu, N. Sun, N. Cui and T. Lu, *Int. J. Biol. Macromol.*, 2021, **183**, 2142–2151.
7 Y. Lu, X. Xu and J. Li, *J. Mater. Chem. B*, 2023, **11**, 3338–3355.

8 A. Dey, P. Bhattacharya and S. Neogi, *Rev. Adhes. Adhes.*, 2020, **8**, 130–152.
9 R. Pinnaratip, M. S. A. Bhuiyan, K. Meyers, R. M. Rajachar and B. P. Lee, *Adv. Healthc. Mater.*, 2019, **8**, 1801568.
10 V. Bhagat and M. L. Becker, *Biomacromolecules*, 2017, **18**, 3009–3039.
11 J. R. Eriksen, J. I. Bech, D. Linnemann and J. Rosenberg, *Hernia*, 2008, **12**, 483–491.
12 H. Quan, O. Liu, L. Zhang and Y. Li, *Molecules*, 2019, **24**, 2586.
13 B. P. Lee, P. B. Messersmith, J. N. Israelachvili and J. H. Waite, *Annu. Rev. Mater. Res.*, 2011, **41**, 99–132.
14 L. Ninan, *Biomaterials*, 2003, **24**, 4091–4099.
15 M. A. North, C. A. Del Grosso and J. J. Wilker, *ACS Appl. Mater. Interfaces*, 2017, **9**, 7866–7872.
16 H. Zhang, L. P. Bré, T. Zhao, Y. Zheng, B. Newland and W. Wang, *Biomaterials*, 2014, **35**, 711–719.
17 C. Cui and W. Liu, *Prog. Polym. Sci.*, 2021, **116**, 101388.
18 G. Dalla Torre, J. I. Mujika, J. I. Lachowicz, M. J. Ramos and X. Lopez, *Dalton Trans.*, 2019, **48**, 6003–6018.
19 J. Kang, S. Zajforoushan Moghaddam and E. Thormann, *Langmuir*, 2023, **39**, 15499–15506.
20 G. Bovone, O. Y. Dudaryeva, B. Marco-Dufort and M. W. Tibbitt, *ACS Biomater. Sci. Eng.*, 2021, **7**, 4048–4076.
21 J. H. Ryu, Y. Lee, W. H. Kong, T. G. Kim, T. G. Park and H. Lee, *Biomacromolecules*, 2011, **12**, 2653–2659.
22 R. Pinnataip and B. P. Lee, *ACS Omega*, 2021, **6**(8), 5113–5118.
23 W. Dou, X. Zeng, S. Zhu, Y. Zhu, H. Liu and S. Li, *Int. J. Mol. Sci.*, 2024, **25**, 9100.
24 Q. Guo, J. Chen, J. Wang, H. Zeng and J. Yu, *Nanoscale*, 2020, **12**, 1307–1324.
25 Z. Zhang and B. P. Lee, *Macromol. Chem. Phys.*, 2025, 70006.
26 S. X. Wang and J. H. Waite, *Nat. Rev. Chem.*, 2025, **9**, 159–172.
27 M. Kim, B. A. Ondrusek, C. Lee, W. G. Douglas and H. Chung, *J. Polym. Sci. Part Polym. Chem.*, 2018, **56**, 1564–1573.
28 M. Lallemang, L. Yu, W. Cai, K. Rischka, A. Hartwig, R. Haag, T. Hugel and B. N. Balzer, *Nanoscale*, 2022, **14**, 3768–3776.
29 H. Tanaka, S. Ito, M. Ojika, T. Nishimaki-Mogami, K. Kondo and K. Wakamatsu, *Int. J. Mol. Sci.*, 2021, **22**, 9145.
30 S.-H. Chen and C.-W. Li, *Front. Chem.*, 2019, **7**, 571.
31 F. Zhu, Z. Sun, Y. Li, C. Chen and Y. Cheng, *Prog. Polym. Sci.*, 2024, **155**, 101857.
32 X. Chen, H. Yuk, J. Wu, C. S. Nabzdyk and X. Zhao, *Proc. Natl. Acad. Sci. U. S. A.*, 2020, **117**, 15497–15503.
33 G. M. Taboada, K. Yang, M. J. N. Pereira, S. S. Liu, Y. Hu, J. M. Karp, N. Artzi and Y. Lee, *Nat. Rev. Mater.*, 2020, **5**, 310–329.
34 G. Tian, Y. Liu, M. Yu, C. Liang, D. Yang, J. Huang, Q. Zhao, W. Zhang, J. Chen, Y. Wang, P. Xu, Z. Liu and D. Qi, *ACS Appl. Mater. Interfaces*, 2022, **14**, 4852–4861.
35 B. Saha, J. Boykin and H. Chung, *J. Am. Chem. Soc.*, 2024, **146**, 23467–23475.
36 S. Nam and D. Mooney, *Chem. Rev.*, 2021, **121**, 11336–11384.
37 A. Rungrod, A. Kapanya, W. Punyodom, R. Molloy, J. Meerak and R. Somsunan, *Biomacromolecules*, 2021, **22**, 3839–3859.
38 F. Rosso, A. Barbarisi, M. Barbarisi, O. Petillo, S. Margarucci, A. Calarco and G. Peluso, *Mater. Sci. Eng., C*, 2003, **23**, 371–376.
39 A. Pourjavadi, Sh Barzegar and F. Zeidabadi, *React. Funct. Polym.*, 2007, **67**, 644–654.
40 K. Nalampang, N. Suebsanit, C. Witthayaprapakorn and R. Molloy, *Chiang Mai J. Sci.*, 2007, **34**(2), 183–189.
41 S. A. Khan, W. Azam, A. Ashames, K. M. Fahelelbom, K. Ullah, A. Mannan and G. Murtaza, *J. Drug Delivery Sci. Technol.*, 2020, **60**, 101970.
42 T. A. Harris-Tryon and E. A. Grice, *Science*, 2022, **376**, 940–945.
43 J. K. Lee, D. B. Kim, J. I. Kim and P. Y. Kim, *Toxicol. In Vitro*, 2000, **14**(4), 345–349.
44 M. Ponec, M. Haverkort, Y. L. Soei, J. Kempenaar and H. Bodde, *J. Pharm. Sci.*, 1990, **79**, 312–316.
45 A. Idrees, V. Chiono, G. Ciardelli, S. Shah, R. Viebahn, X. Zhang and J. Salber, *Int. J. Artif. Organs*, 2018, **41**, 779–788.
46 T. Søeborg, L. H. Basse and B. Halling-Sørensen, *Toxicology*, 2007, **236**, 140–148.
47 M. Nakamura, T. Rikimaru, T. Yano, K. G. Moore, P. J. Pula, B. H. Schofield and A. M. Dannaenberg Jr, *J. Invest. Dermatol.*, 1990, **95**(3), 325–332.
48 F. Benavides, T. M. Oberyszyn, A. M. VanBuskirk, V. E. Reeve and D. F. Kusewitt, *J. Dermatol. Sci.*, 2009, **53**, 10–18.
49 J. A. Klun, A. Khrimian, E. Rowton, M. Kramer and M. Debboun, *J. Med. Entomol.*, 2006, **43**, 1248–1251.
50 M. Guvendiren, P. B. Messersmith and K. R. Shull, *Biomacromolecules*, 2008, **9**, 122–128.
51 Y. Ai, J. Nie, G. Wu and D. Yang, *J. Appl. Polym. Sci.*, 2014, **131**, app.41102.
52 C. Creton and L. Leibler, *J. Polym. Sci., Part B: Polym. Phys.*, 1996, **34**, 545–554.
53 K. Chen, Q. Lin, L. Wang, Z. Zhuang, Y. Zhang, D. Huang and H. Wang, *ACS Appl. Mater. Interfaces*, 2021, **13**, 9748–9761.
54 M. Okada, E. S. Hara, A. Yabe, K. Okada, Y. Shibata, Y. Torii, T. Nakano and T. Matsumoto, *Adv. Mater. Interfaces*, 2020, **7**, 1902089.
55 R. Kong and R. Bhargava, *Analyst*, 2011, **136**, 2359.
56 M. E. Tumbleson and L. B. Schook, *Advances in Swine in Biomedical Research*, Plenum Press, New York London, 1st edn, 1996.
57 X. Zeng, S. Liu, Z. Shi and B. Xu, *Org. Lett.*, 2016, **18**, 4770–4773.
58 L. Fernández-Vega-Cueto, M. Persinal-Medina, N. Vázquez, M. Chacón, B. Alfonso-Bartolozzi, S. Alonso-Alonso, T. Sánchez, S. Berisa-Prado, L. M. Martínez-López, J. Merayo-Lloves and Á. Meana, *Pharmaceutics*, 2022, **14**, 2325.
59 Y. Son, E. O. N. Phillips, K. M. Price, L. Z. Rosenberg, B. Stefanovic, C. M. Wolfe, T. S. Shaath, A. Om,

G. F. Cohen and A. Gunjan, *J. Am. Acad. Dermatol.*, 2020, **83**, 1304–1314.
60 A. Phillips, T. Bullock and N. Plant, *Toxicology*, 2003, **192**, 219–227.
61 L.-F. Seet, L. Z. Toh, S. N. Finger, S. W. L. Chu, B. Stefanovic and T. T. Wong, *J. Mol. Med.*, 2016, **94**, 321–334.
62 T. Harper, R. Slegeris, I. Pramudya and H. Chung, *ACS Appl. Mater. Interfaces*, 2017, **9**, 1830–1839.